Supplementary Information

OAPS-based PI aerogels used as antenna substrate in extreme environments

Man Zhang,[a] Dezhi Wang,[a] Qing Zhu,[c] Yupeng Liu,[b] Tingting Jia,[c]Jiajia Zou,[d] Wen Yang,[c] Zhen Fan,[e] Liwei Zhao,[a] Hongfeng Li,[a] Pan Wang,[a] Hao Feng,[a] Kai Su,[a] Shuai Zheng,[a]* Changwei Liu[a]*

[a] Institute of PetroChemistry, Heilongjiang Academy of Science, Harbin 150040, China

[b] School of Materials Science and Chemical Engineering, Harbin University of Science and Technology, Harbin 150080, China

[c] College of Materials Science and Chemical Engineering, Harbin Engineering University, Harbin, 150001, China

[d] The 38th Research Institute of China Electronics Technology Group Corporation, Anhui 230088, China

[e] College of Science, Northeastern University, Shenyang,110819, China

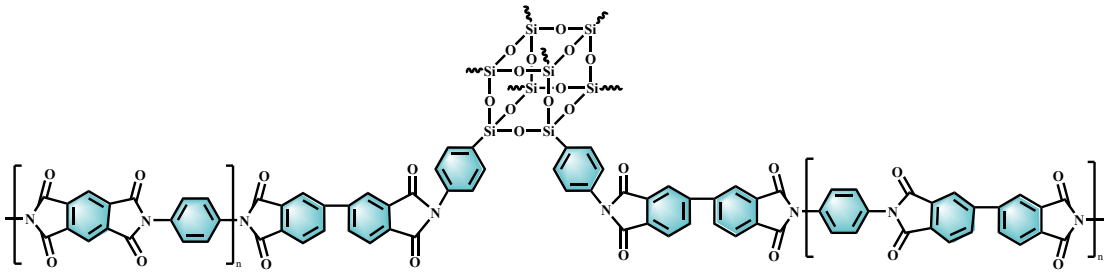

Fig. S1 The structure of PI/OAPS-n hybrid aerogels after imidization

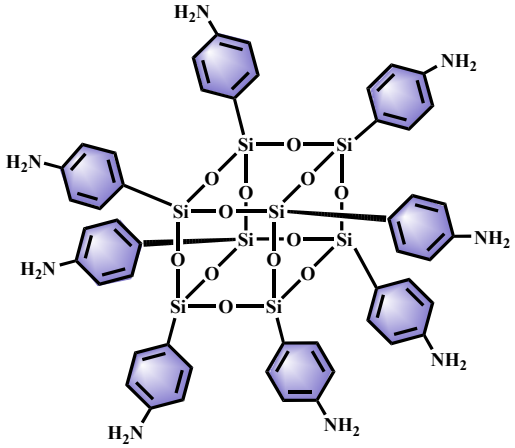

Fig. S2 The molecular structure of OAPS, which resembles an octopus structure

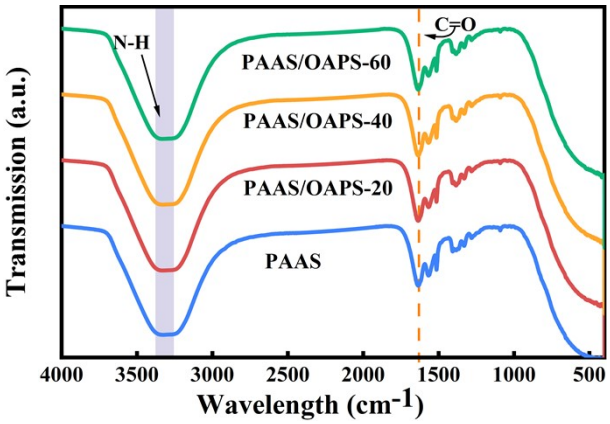

Fig. S3 FTIR spectra of PAAS and PAAS/OAPS-n

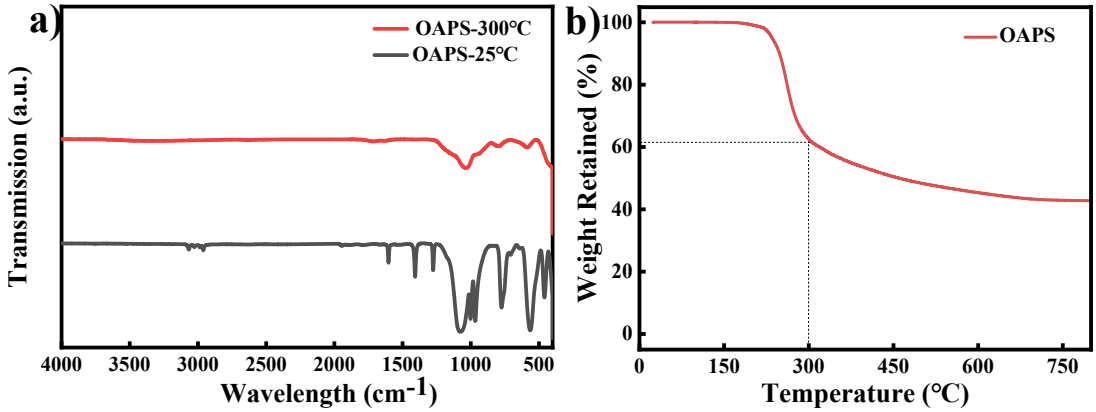

Fig. S4 a) FTIR spectra of OAPS and OAPS after thermal treatment; b) TGA of OAPS

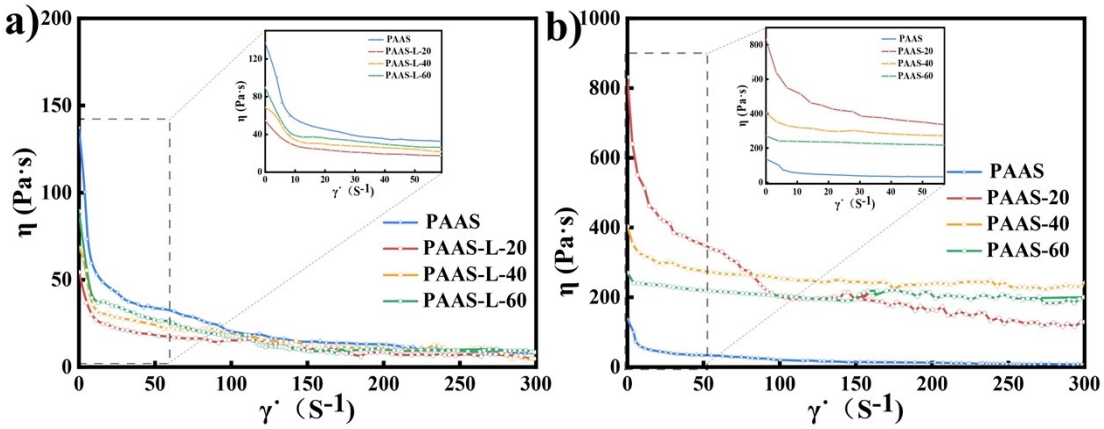

Fig. S5 rheological characterizations：a) Linear PAAS; b) OAPS-containing PAAS

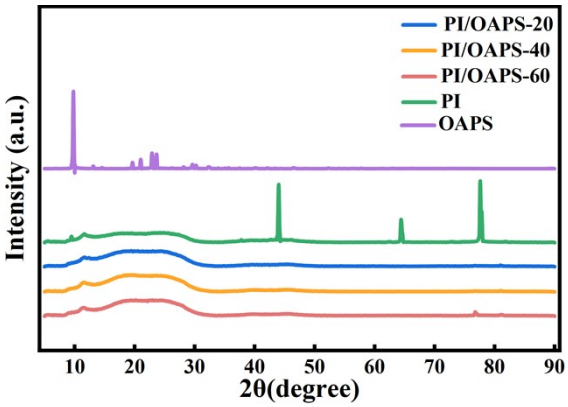

Fig. S6 XRD patterns of PI and PI/OAPS-n

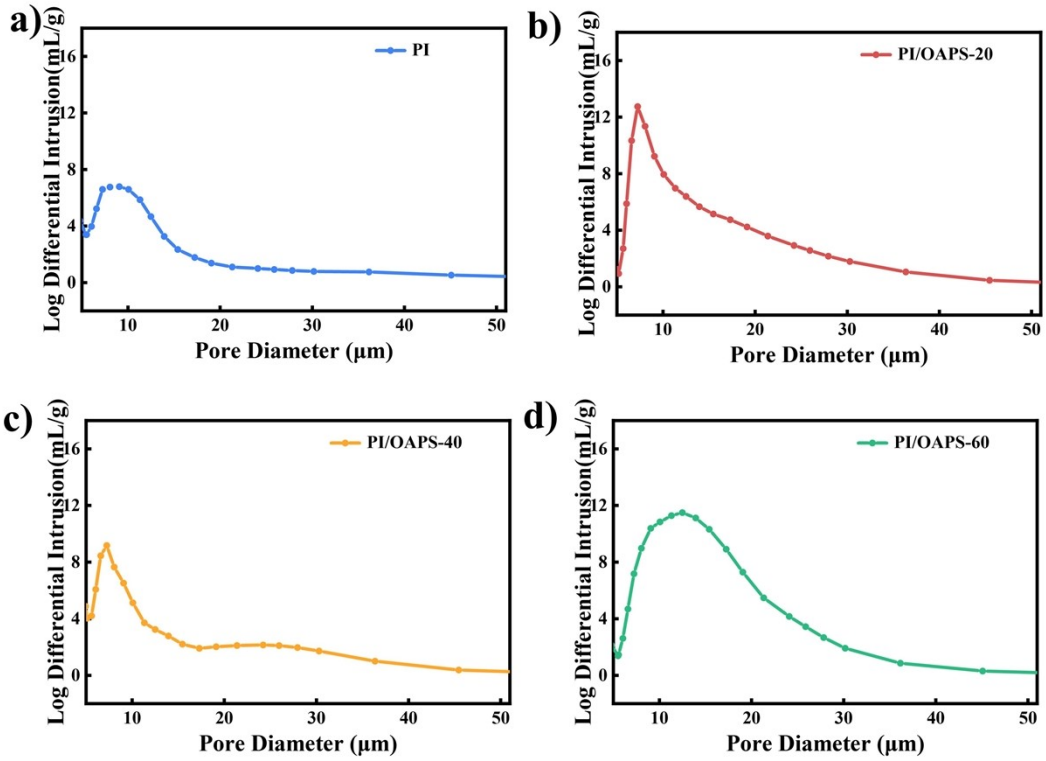

Fig. S7 Pore size distribution plots of PI and PI/OAPS-n

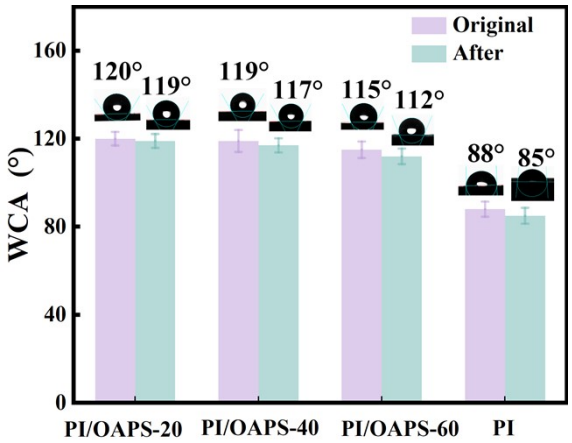

Fig. S8 Contact angles of PI and PI/OAPS-n before and after damp-heat aging at

85 °C and 85 % RH for 168 h

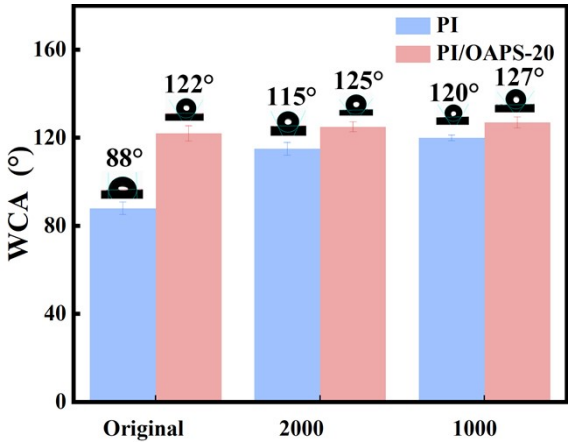

Fig. S9 Contact angles of PI and PI/OAPS-20 before and after sanding with sandpapers of different grit sizes.

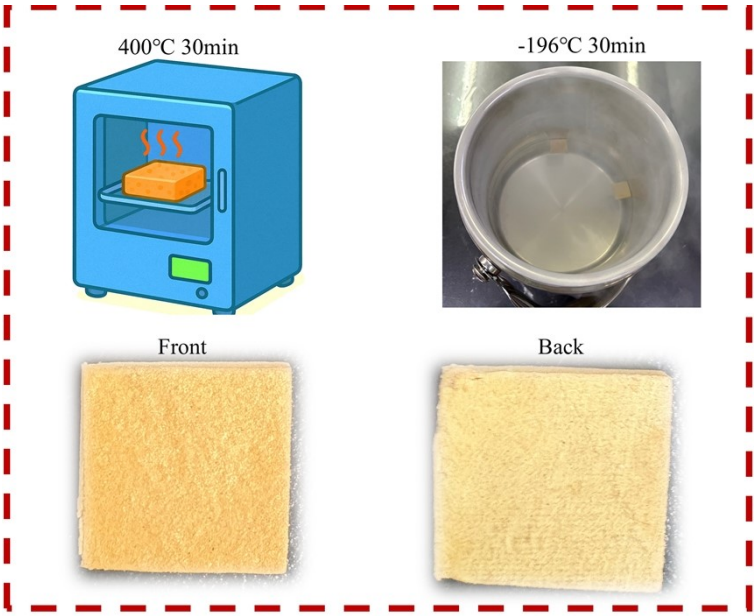

Fig. S10 Macroscopic structure of the PI/OAPS-20 aerogel following thermal shock tests

Table 1 Physical Properties of PI and PI/OAPS-n

Sample	Shrinkage Rate (%)	Density（g/cm^3）	Porosity (%)
PI/OAPS-20	22.4±0.433	0.128±0.003	90.541±0.282
PI/OAPS-40	22.7±0.358	0.131±0.005	90.017±0.905
PI/OAPS-60	23.2±0. 426	0.133±0.003	89.340±0.327
PI	32.9±0.460	0.142±0.003	88.628±0.400

Table 2: Pore structure parameters of the PI and PI/OAPS-n by MIP.

Sample	Median pore	Mode pore	Total pore area

	diameter(volume) (μm)	diameter(μm)	(m^2/g)
PI/OAPS-20	7.737	7.176	14.681
PI/OAPS-40	6.117	7.168	14.196
PI/OAPS-60	10.178	12.52	9.371
PI	6.182	8.655	11.396

Table 3 Physical Properties of PI and PI/OAPS-n of different batches

Sample	Shrinkage Rate (%)	Density（g/cm^3）	Porosity (%)
PI/OAPS-20	22.7±0.465	0.128±0.002	91.127±0.328
PI/OAPS-40	23.5±0.384	0.131±0.004	90.674±0.781
PI/OAPS-60	24.3±0.436	0.133±0.004	89.749±0.379
PI	33.8±0.453	0.142±0.002	88.870±0.448

Table 4 Physical Properties of PI and PI/OAPS-n of different batches

Sample	Shrinkage Rate (%)	Density（g/cm^3）	Porosity (%)
PI/OAPS-20	21.8±0.447	0.128±0.003	90.269±0.369
PI/OAPS-40	22.4±0.369	0.131±0.002	89.866±0.514
PI/OAPS-60	23.0±0. 411	0.133±0.003	89.111±0.398
PI	32.3±0.472	0.142±0.004	88.158±0.377

Table 5 Thermal, mechanical, surface, and dielectric properties of PI and PI/OAPS-n

Sample	$T_{d5\%}$ (°C)	Storage Modulus (E') (°C)	T_g (°C)	Contact Angle (°)	Dielectric Constant D_k	Dielectric Loss D_f (×10^-3)
PI/OAPS-20	602	187.90	332.08	120.02	1.08±0.005	1.28±0.132
PI/OAPS-40	592	197.65	331.11	118.64	1.10±0.00	1.12±0.013

					3	
PI/OAPS-60	603	162.95	350.98	114.65	1.11±0.003	1.37±0.071
PI	597	150.12	352.35	87.63	1.24±0.009	3.12±0.24

Table 6 Thermal, mechanical, surface, and dielectric properties of PI and PI/OAPS-n of different batches

Sample	**Dielectric Constant 2** D_k	**Dielectric Loss 2** D_f **(×10^-3)**	**Dielectric Constant 3** D_k	**Dielectric Loss 3** D_f **(×10^-3)**
PI/OAPS-20	1.08±0.004	1.46±0.112	1.09±0.006	1.18±0.29
PI/OAPS-40	1.10±0.003	1.79±0.0143	1.11±0.004	1.19±0.28
PI/OAPS-60	1.11±0.004	1.88±0.111	1.11±0.005	1.42±0.12
PI	1.25±0.006	3.67±0.26	1.22±0.006	3.53±0.15